

ANALYSIS OF FACTORS INFLUENCING HEAT TRANSFER PERFORMANCE BASED ON SHIP SPRAY COOLING SYSTEM

by

Yujiao WANG* and Long HUANG

College of Marine Electrical and Intelligent Engineering, Jiangsu Maritime Institute,
Nanjing, China

Original scientific paper
<https://doi.org/10.2298/TSCI231015288W>

The increasingly prominent issue of equipment heat dissipation has seriously hindered the further development of ship engineering. The heat exchange of traditional heat dissipation technology is limited, resulting in insufficient heat dissipation capacity and difficulty in meeting the heat dissipation needs of ships. Given these problems, this study constructs to use spray cooling technology to solve the heat dissipation problem of ships, and on this basis, the reason causing the heat transfer performance of R134a spray cooling system are analyzed. As there is lubricating oil in the spray cooling system, this study also partially explores such type of system with lubricating oil. The experimental data validate that when the heat flux densities are 30.0 W/cm², 45.0 W/cm², and 55.0 W/cm², the heat transfer coefficients are 19.23×10³ W/m²°C, 24.02×10³ W/m²°C, and 18.70×10³ W/m²°C, respectively, and the surface temperature of the heat source is 29.13 °C, 38.21 °C, and 48.23 °C. When the lubricating oil concentration is fixed at 1.47%, during the process of increasing the heat flux density from 10 W/cm² to 50 W/cm², the surface temperature rises from 32.33 °C to 55.28 °C, and the heat transfer coefficient increases from 7.54×10³ W/m²°C to 9.46×10³ W/m²°C. In conclusion, the proposed mass-flow rate, heat flow density, and evaporation chamber pressure have a significant impact on the heat transfer performance of the ship's spray cooling system, on the contrary, the lubricating oil has a significant impact on the system performance.

Key words: *degree of supercooling, spray cooling system, heat transfer coefficient, surface temperature of the heat source, R134a spray system*

Introduction

In the current shipping industry, the efficiency and sustainability of ship power systems have become the core concerns of research. As an important technical means to improve the efficiency of power system, Marine spray cooling system (SCS) has attracted wide attention. Under different sailing and climatic conditions, the heat transfer performance (HTP) of the system involves many complex factors, and it is very important to study these factors deeply for the optimization and performance improvement of the system. Previous studies have shown that ship operating state and surrounding environmental conditions directly affect the heat

*Corresponding author, email: 15851831577@163.com

transfer process of SCS [1, 2]. In naval engineering, equipment generates significant heat during operation, risking overheating, reduced efficiency, and malfunctions without proper heat dissipation [3, 4]. Conventional methods using air and water for natural and forced convection fall short in meeting the heat dissipation needs of miniaturized, high-power ship equipment with elevated heat flux [5, 6].

Therefore, this study designs to use the SCS to heat the ship equipment [7]. The SCS is a practical solution for high-power and high heat flux heat dissipation. It involves spraying liquid onto the heat source (SoHS), rapidly reducing its temperature through evaporation and heat absorption. The SCS offers high heat transfer efficiency (HTE) and dissipation ability. The injection process ensures uniform droplet distribution, minimal cooling medium demand, no boiling hysteresis, and low contact thermal resistance with equipment surfaces, making it a focus of scholarly attention. This study examines factors influencing SCS HTP on ships, using R134a refrigerant. It explores the spray process and heat transfer mechanism, considering variables and the impact of lubricating oil in ship SCS. The aim is to experimentally assess common factors affecting SCS HTP on ships, providing practical insights for spray cooling technology (SCT) application. This study introduces two main innovations. Firstly, it establishes a closed SCS using R134a refrigerant to explore the effects of mass-flow, heat density, under-cooling, and spray chamber evaporation pressure on HTP. Secondly, it designs a refueling device to examine the influence of lubricating oil concentration (LOC) on SCS by adjusting the flow rate based on heat flux density (*HFd*).

Related works

Heat dissipation technology (HDT) refers to the effective transfer, dispersion, or discharge of heat from an object or system to the surrounding environment through various methods. Many scholars have conducted in-depth discussions on the research and application of HDT. Wang *et al.* [8] designed a circulating hollow shaft oil cooling (HSOC) structure for high-speed permanent magnet synchronous motors. They studied convective heat transfer (CHT) characteristics by analyzing fluid dynamics. The cyclic HSOC showed a higher CHT coefficient than direct HSOC, suggesting it effectively dissipates heat, enhances equipment efficiency, and prolongs service life. Liu *et al.* [9] proposed an open micro-channel heat sink with transverse ribs to improve heat transfer for a W/Cu flat plate model. Their aim was to meet heat dissipation requirements for future fusion reactors with high heat loads. Numerical studies on the fluid-flow and heat transfer of IMHS indicated significant improvement, reducing average wall temperature by 19.6 K and maximum surface temperature by 30.6 K. Clark *et al.* [10] studied pressure drop oscillation's impact on heat transfer in a micro-channel cut into copper radiators. Analyzing steady-state data and high-frequency pressure signals, they aimed to enhance micro-channel heat sink performance. The findings showed that pressure drop oscillation improves flow mixing and heat load distribution, increasing heat transfer surface utilization. Klinkhamer *et al.* [11] suggested jet cooling technology for electric vehicle equipment, particularly when traditional cooling methods reach their limits. Jet cooling involves driving cooling liquid through an injection device to spray high-speed fluid on the object for effective heat exchange, proven successful in automotive cooling applications.

As a new cooling technology, spray cooling mainly absorbs and dissipates heat quickly by spraying tiny water droplets on the equipment surface, thus effectively reducing the equipment temperature. Many scientists have also discussed the factors influencing the HTP of spray cooling. Wu *et al.* [12] conducted a theoretical analysis on the HTP of SCT to balance the temperature uniformity and battery compactness. The effect of spray cooling on the

management system at a highly discharging rate was studied experimentally. In the cooling mode with SCS as 4+2.5 m/s, the total heat transfer coefficient (HTC) reached 201.0 W/m²K, which exceeds 409.3% than the HTC of forced air-cooling. Additionally, the difference between the spray concentration on the heat source surface and that in the mainstream area is essential for affecting the HTP of spray cooling. Chang *et al.* [13] investigated water nanofluid spray cooling at various super-cooling temperatures. Using under-cooled 20 °C nanofluids resulted in HTC approximately 8.3% to 15.6% higher compared to other temperatures. They observed a decrease in HTP with longer spraying times. Huang *et al.* [14] examined the impact of different surface types on spray cooling. Changes in roughness didn't significantly affect HTC. Compared to smooth surfaces, super-hydrophilic and super-hydrophobic surfaces decreased HTC by 9.6% and 9.2%, respectively.

From aforementioned, many experts have discussed factors affecting HTP in HDT and spray cooling, but for ship equipment with high power and heat flux, current heat dissipation capacity and HTE are inadequate due to small working medium flow rates. Existing analyses of SCS HTP often focus on heat transfer surfaces and sub-cooling, neglecting the influence of *MFr*, evaporation chamber pressure (*ECp*), and *HFd*. This study addresses these issues, exploring the impact of *MFr*, *HFd*, under-cooling, and *ECp* on R134a SCS HTP. Additionally, a refueling device is introduced to analyze lubricating oil effects on HTP considering oil content, *MFr*, and *HFd*.

Heat transfer performance based on ship spray cooling system

Ship SCS is a common cooling method for ship equipment. It lowers equipment surface temperature by spraying water in a mist, facilitating heat exchange. This chapter focuses on ship SCS's spray process, heat transfer mechanism, and studies the HTP of R134a refrigerant and lubricating oil on ship SCS.

Spray process and heat transfer mechanism of ship spray cooling system

Ships, serving purposes such as transportation and combat, generate substantial thermal energy from prolonged equipment operation [15]. If not dissipated promptly, this heat can cause overheating, leading to performance issues and damage. Hence, ships necessitate cooling systems, expressed by:

$$Q = \beta A (T_{\text{sur}} - T_f) \quad (1)$$

where Q is the heat dissipation amount of the device, β and A – the HTC and heat transfer area, and T_{sur} and T_f – the surface temperature and fluid temperature of the heat exchange surface, respectively. Traditional ship cooling methods, like water cooling and air conditioning, pose issues like performance impact and high energy consumption [16-18]. Addressing these drawbacks, SCT was introduced. The SCT involves atomizing the cooling medium into droplets through a nozzle, sprayed onto the heat exchange surface. This creates a liquid film, aiding heat removal through convection, phase change, nucleating boiling, and secondary nucleation (2Nu). The SCS structure is simple and applicable, categorized into open and closed systems, fig. 1.

Figures 1(a) and 1(b) display open and closed cycle systems. The choice depends on the environment and coolant. Using water in an open system reduces energy use and is cost-effective. For Freon, a closed system is vital to cut emissions. In SCS, the nozzle is crucial for cooling; it varies based on the type, either pressure atomizing or air-assisted, fig. 2.

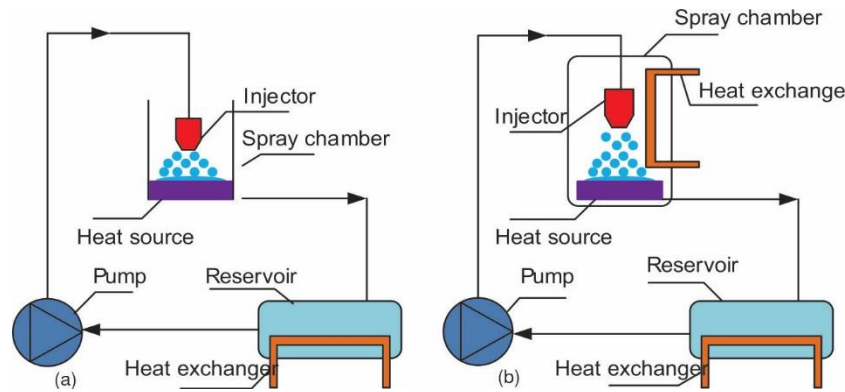


Figure 1. Schematic diagram of SCS structure; (a) open circulation system and (b) closed circulation system

Figure 2(a) shows a gas-assisted atomization nozzle using high-pressure air to create small liquid droplets. In contrast, fig. 2(b) presents a pressure atomizing nozzle that uses high-pressure liquid to atomize through small nozzle holes. This system includes a nozzle, nozzle seat, and liquid supply to produce consistent droplets. In this study, a pressure atomizing nozzle with an internally etched micro-channel was chosen. When spraying droplets on the SoHS, some bounce off, forming smaller droplets, while others stick to create a liquid film, fig. 3.

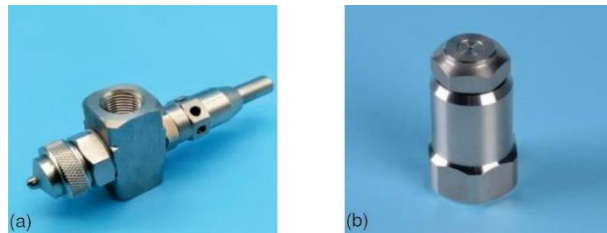


Figure 2. Two different nozzle types; (a) air-assisted atomizing nozzle and (b) pressure atomizing nozzle

In fig. 3, the variation of the droplet after spraying onto the SoHS mainly depends on the Weber number of the droplet. When Weber number is less than a certain critical value, the droplets will rebound. Weber number is the ratio of the inertial force and surface tension of the droplet, as shown in:

$$We = \frac{\rho v^2 s}{\sigma} \quad (2)$$

where ρ and v represent fluid density and droplet rate, respectively, s – the average diameter of the droplet, and σ – the surface tension coefficient of the droplet. Droplet adhesion to the SoHS during collision depends on the Sommerfeld number. When the Sommerfeld number ranges from 3 to 57.7, droplets adhere to the surface upon contact, forming a liquid film. The definition of Sommerfeld number, $\alpha_{\text{Sommerfeld}}$, is:

$$\alpha_{\text{Sommerfeld}} = We^{0.5} Re^{0.25} \quad (3)$$

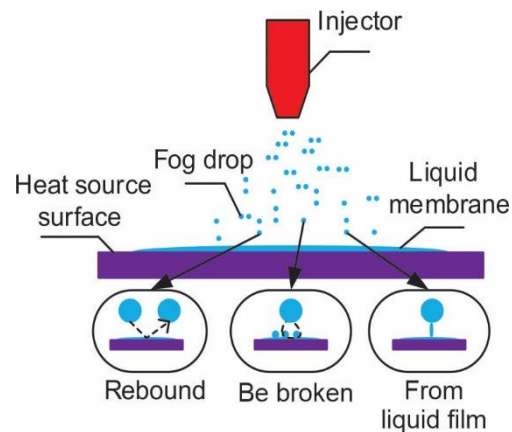


Figure 3. Schematic diagram of droplet impact process

where Re is the Reynolds number of the droplet, as expressed in:

$$Re = \frac{\rho v s}{\eta} \quad (4)$$

where η is the dynamic viscosity coefficient of the droplet. Spray cooling involves two heat transfer mechanisms. Some of the cooling medium sprayed on the SoHS does not change phase and removes heat through CHT, without boiling. The rest undergoes a phase change when heated, extracting heat through boiling heat transfer (BHT). In summary, the heat transfer mechanism of spray cooling consists of these four modes: CHT and BHT, forced CHT, liquid film evaporation (LFE), nucleate boiling, and 2Nu BHT, as shown in fig. 4.

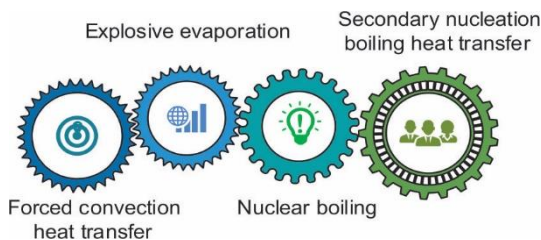


Figure 4. Four heat transfer modes in spray cooling heat transfer mechanism

In fig. 4, forced convection starts when a spray droplet attaches to a hot surface, forming a thin liquid film that conducts heat. The LFE follows, as the droplet quickly evaporates, absorbing heat and cooling the surface. This enhances heat transfer enhancement by generating steam. Nucleation boiling occurs when the droplet's surface temperature exceeds the saturation temperature, forming bubbles that carry away heat, improving cooling. The 2Nu boiling heat transfer (2Nu

BHT) involves bubbles detaching, creating a cloud that enhances boiling on the droplet's surface.

Heat transfer performance of R134a ship's spray cooling system

Warship SCS design considers droplet specifics, cooling medium traits, and surface features for spray cooling. Selecting a cooling substance involves factors like heat capacity, electrical insulation, safety, and non-corrosiveness. Keeping ship equipment at optimal temperatures is crucial to avoid problems like overheating and stress. Table 1 lists physical properties of common cooling fluids.

Table 1. Physical properties of common cooling working fluid

Cooling working medium	Boiling point [°C]	Latent heat of vaporization (LHV) [kJkg ⁻¹]	Density [kgm ⁻³]	Toxicity	Inflammability
Water	100.0	2256	1000	No	No
Methyl alcohol	64.7	1109	791	Yes	Yes
Ethanol	78.0	849	800	No	Yes
R134a	-26.1	217	1376	No	No

In tab. 1, R134a refrigerant is a medium to low temperature environmentally friendly refrigerant, which is composed of colorless, odorless, and non-toxic fluoroalkane compounds. The R134a refrigerant has an ozone destroying potential value of 0, and its boiling point and LHV are -26.1 °C and 217 kJ/kg, respectively. The R134a was chosen as the cooling medium due to its excellent overall performance, offering efficient refrigeration in medium to low temperature settings. The closed SCS structure using R134a refrigerant as the cooling working fluid is fig. 5.

In fig. 5, the R134a refrigerant is atomized in the nozzle through different cross sections and sprayed onto the SoHS for heat exchange. In this study, the heat conduction is simplified as a 1-D axial problem, and the radial heat conduction is ignored. A thermocouple measures the temperature to obtain HFd , as shown in:

$$q = \lambda \frac{T_2 - T_1}{h_1} \quad (5)$$

where T_2 and T_1 represent the temperature values of measuring Points 2 and 1 in fig. 5, respectively, h_1 – the distance between measuring points T_2 and T_1 in fig. 5, and λ – the TC of red copper. The calculation of the T_{sur} of the heat source is:

$$T_{sur} = T_1 - \frac{qh_0}{\lambda} \quad (6)$$

where h_0 is the distance between the measurement point T_1 and the SoHS, so the calculation of the HTC is:

$$\beta = \frac{q}{T_{sur} - T_{sat}} \quad (7)$$

where T_{sat} is the evaporation temperature of the spray chamber. The measurement error of the thermocouple is ± 0.1 °C. The measurement error of the distance between adjacent thermocouples is ± 0.02 mm. Therefore, the relative error value φ_q of HFd q is calculated using:

$$\varphi_q = \sqrt{\left(\frac{\partial \ln q}{\partial T_1}\right) \Delta T_1^2 + \left(\frac{\partial \ln q}{\partial T_2}\right) \Delta T_2^2 + \left(\frac{\partial \ln q}{\partial h_1}\right) \Delta h_1^2} \quad (8)$$

where ΔT_1 and ΔT_2 represent the measurement errors of T_1 and T_2 , Δh_1 – the measurement error of the distance between T_1 and T_2 measurement points. The relative error value φ_T of the T_{sur} of the heat source is solved as:

$$\varphi_T = \sqrt{\left(\frac{\partial \ln T_{sur}}{\partial T_1}\right) \Delta T_1^2 + \left(\frac{\partial \ln T_{sur}}{\partial T_2}\right) \Delta T_2^2 + \left(\frac{\partial \ln T_{sur}}{\partial h_0}\right) \Delta h_0^2 + \left(\frac{\partial \ln T_{sur}}{\partial h_1}\right) \Delta h_1^2} \quad (9)$$

where Δh_0 is the measurement error of the distance between measuring point T_1 and the SoHS. The calculation of the relative error value φ_β of the HTC β is:

$$\varphi_\beta = \pm \left(\left| \varphi_q \right| - \left(\left| \frac{T_{sur}}{T_{sur} - T_{sat}} \varphi_T \right| + \left| \frac{T_{sat}}{T_{sur} - T_{sat}} \varphi_{T_s} \right| \right) \right) \quad (10)$$

where φ_{T_s} is the relative error of T_{sat} and the expression of φ_{T_s} is:

$$\varphi_{T_s} = \frac{1}{m} \sum_{i=1}^{10} \left(\frac{\Delta T_{sat,i}}{T_w} \right) \quad (11)$$

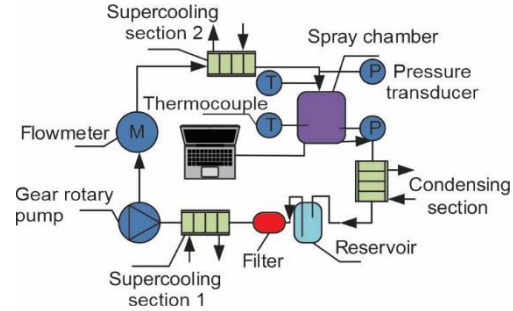


Figure 5. Schematic diagram of R134a SCS

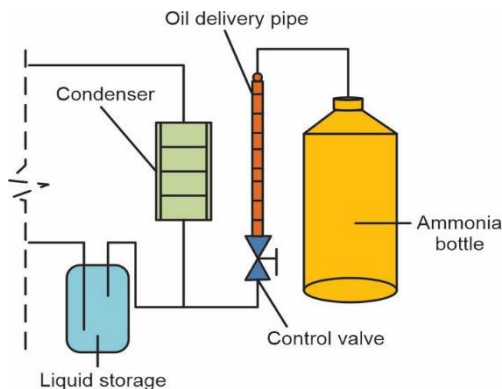


Figure 6. Schematic diagram of refueling device

where m is the number of measurements, T_w – the average evaporation temperature obtained after multiple measurements, and $\Delta T_{\text{sat},i}$ – the relative deviation generated by each measured evaporation temperature. In R134a SCS, pumps and auxiliary chillers are replaced by compressors, which may contain lubricating oil. This oil can impact SCS performance. To test the effect of LOC on HTP under various MFR s and HFD , a refueling device was added to the existing SCS, as depicted in fig. 6.

Analysis of heat transfer performance results of ship spray cooling system

Figure 6 displays a refueling set-up with a valve, oil pipeline, and high-pressure ammonia cylinder. During refueling, ammonia flow and pressure are managed, and after refueling, the valve is shut and the oil pipeline disconnected. The lubricating oil, RH68L, is used with R134a refrigerant. To charge the system, vacuum, inject R134a, close the valve, add oil without bubbles, and connect the oil pipe to the ammonia cylinder. The oil is then injected into the SCS in 10 parts at slightly higher pressure.

The T_{sur} and HTC-HS are important indicators to measure the HTP strength of the ship's SCS. Therefore, this chapter focuses on the influence of sub-cooling, MFR of working medium, HFD and ECp of spray chamber on the HTP of R134a SCS. To analyze the impact of lubricating oil on the HTP of SCS, the changes in T_{sur} and heat source HTC of SCS are studied under different LOC, MFR s, and HFD .

Analysis of factors influencing the HTP of R134a spray cooling system

To verify the effectiveness of the proposed HTC calculation value, the first step is to set the HFD to 30.0 W/cm² and the under-cooling to 3.0 °C, and only change the MFR to obtain the HTC. Thus, judgment can be made based on the comparison between the theoretical calculation of the HTC and the actual values.

From fig. 7(a) and 7(b), when the MFR is 1 kg per hour, the theoretical calculated value of the HTC is 18.11×10^3 W/m²°C, the actual value is 17.29×10^3 W/m²°C, and the error and relative error are 0.82×10^3 W/m²°C and 4.74%, respectively. When the MFR is 6 kg per hour the theoretical and actual values of the HTC are 19.98×10^3 W/m²°C and 19.01×10^3 W/m²°C, respectively, with an error of 0.97×10^3 W/m²°C and a relative error of 5.10%. Figure 7 shows good agreement between calculated and experimental HTC values (max relative error < 15%), validating the proposed HTC calculation. Subsequent experiments vary the cooling water flow (MFR) to study its impact on R134a SCS HTP, keeping HFD and under-cooling constant at 40.0 W/cm² and 3.0 °C, respectively.

In fig. 8(a), when the MFR is 1 kg per hour, the ST-HS and HTC-HS are 48.70 °C and 10.12×10^3 W/m²°C, respectively. When the MFR reaches 6 kg per hour, the ST-HS is 31.5 °C, and the HTC is 20.01×10^3 W/m²°C. From fig. 8(b), since the pressure of spray chamber is determined by heat flux, mass-flow and under-cooling, when the under-cooling and heat flux

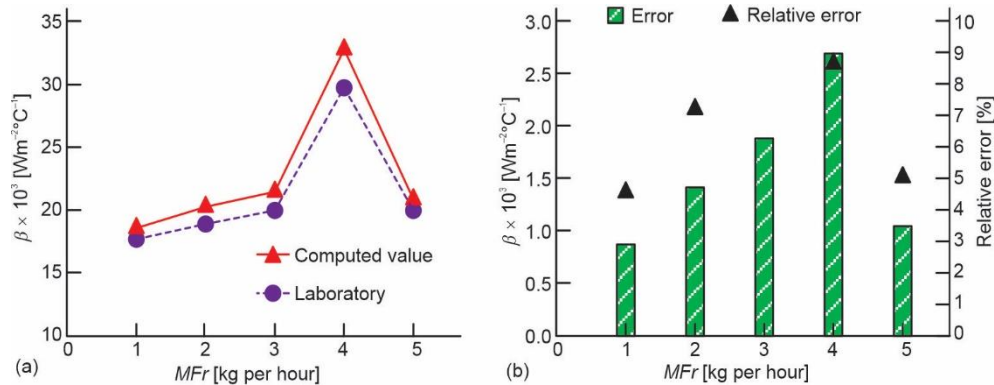


Figure 7. Theoretical calculation and experimental results of HTC; (a) comparing the calculated value with the experimental value and (b) error and relative error

are kept constant, the pressure change law of spray chamber is connected with the ST-HS. When the *MFr* is 1 kg per hour, the pressure of spray chamber is 405.01 kPa. When the *MFr* is 6 kg per hour, the pressure of spray chamber is 347.23 kPa. In fig. 8, increasing the cooling medium flow (*MFr*) improves HTE by cooling the surface with more droplet spraying. However, there's a challenge as the upper liquid film hinders lower film evaporation, especially with accumulated droplets. When *MFr* reaches 4 kg per hour, the HTP of R134a SCS gradually decreases. Following experiments explore how changing *Hfd* affects HTP, while maintaining *MFr* and under-cooling at 3.0 kg per hour.

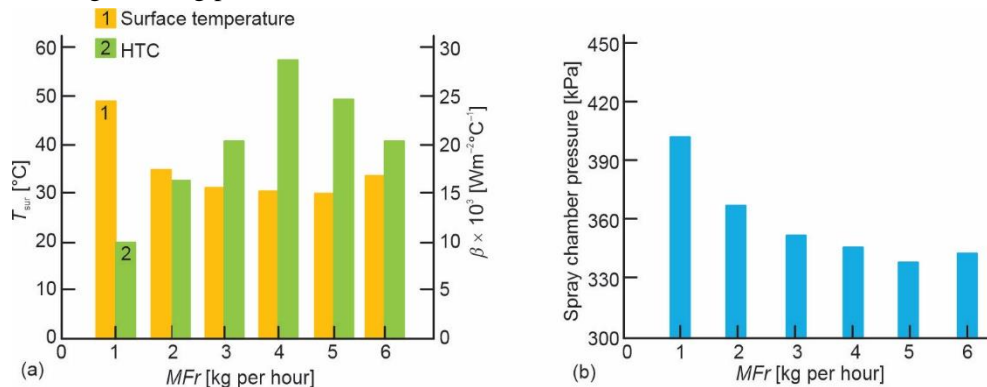


Figure 8. Effect of *MFr* on HTP; (a) influence of *MFr* on surface temperature and HCT of heat source and (b) pressure in the spray chamber changes with the mass flow

In fig. 9(a), when the *Hfd* increases from 30.0 W/cm² to 55.0 W/cm², the ST-HS continues to rise, from 29.13 °C to 48.23 °C. The HTC shows a tendency of first increasing and then decreasing. When the *Hfd* increases from 30.0 W/cm² to 45.0 W/cm², the HTC increases from 19.23×10^3 W/m²°C to 24.02×10^3 W/m²°C. But when the *Hfd* increases to 55.0 W/cm², the HTC decreases to 18.70×10^3 W/m²°C. Figure 9(b) shows the change of spray chamber pressure with heat flux. The trend of its change is consistent with the trend of the ST-HS. When the heat flux is 30.0 W/cm² and 55.0 W/cm², respectively, the pressure of spray chamber is 351.23 kPa and 42.12 kPa, respectively. Figure 9 shows that as the *Hfd* increases, the SoHS continues to rise. Increasing droplet evaporation thins the liquid film, reducing the upper film's blocking effect, lowering thermal resistance, and increasing HTC. At *Hfd* 45.0 W/cm², the

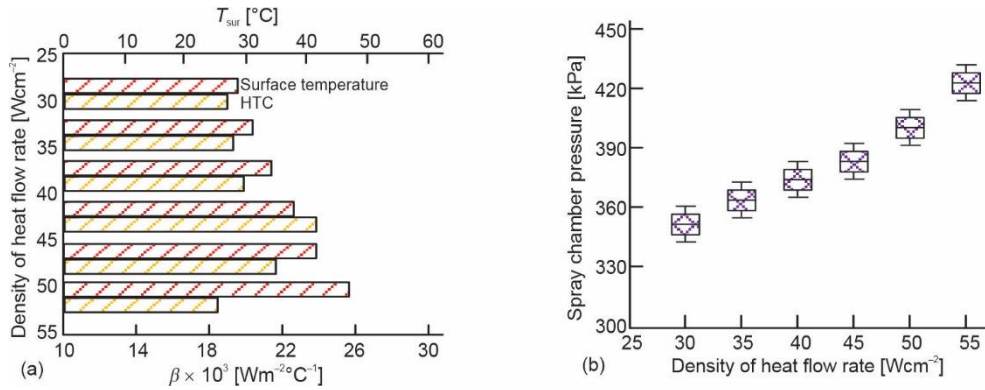


Figure 9. Effect of *HfD* on HTP; (a) influence of *HfD* on surface temperature and HTC of heat source and (b) pressure in the spray chamber changes with the *HfD*

upper liquid film on SoHS is thin and just wet, resulting in the highest HTP. Further *HfD* increase causes excessive droplet evaporation, leading to local drying of SoHS and a reduction in HTP. To study sub-cooling's impact on SCS HTP, *MFr* and heat density were set at 3.0 W/cm² and 50.0 W/cm², respectively, with only sub-cooling varied. Table 2 presents the experimental results.

Table 2. Influence of cooling degree on HTP

Influencing factor	0 °C	1 °C	2 °C	3 °C	4 °C	5 °C	6 °C
ST-HS [°C]	39.24	39.17	38.89	38.64	38.47	38.25	38.01
HTC × 10 ³ [Wm ⁻² C ⁻¹]	19.01	19.18	19.26	19.45	19.67	19.91	20.13
Spray chamber pressure [kPa]	370.12	369.47	368.84	368.22	367.66	367.01	366.43

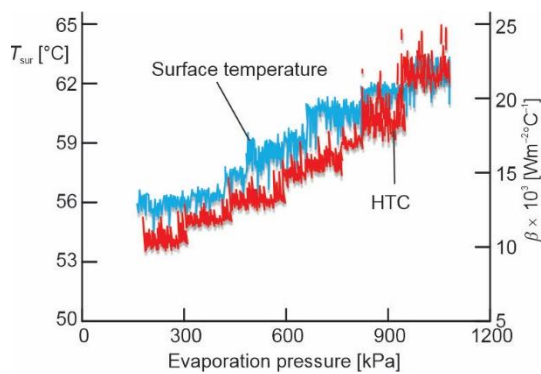


Figure 10. Effect of *ECp* in spray chamber on HTP

increases from 56.01 °C to 62.03 °C, and the HTC increases from 11.23 × 10³ W/m²C to 22.47 × 10³ W/m²C. Increasing the *ECp* slows down liquid working fluid evaporation, raising ST-HS and HTC-HS, thereby improving SCS HTP.

In tab. 2, when the under-cooling increases from 0 °C to 6 °C, the ST-HS only decreases by about 1.23 °C. The HTC increased from 19.01 × 10³ W/m²C to 20.13 × 10³ W/m²C, and the pressure of spray chamber slightly decreased by 3.69 kPa. The data in tab. 2 indicate that simply increasing the sub-cooling does not significantly reduce the ST-HS and increase the HTC, thereby not significantly improving the HTP of SCS.

In fig. 10, when the under-cooling, *MFr*, and *HfD* are set at 3.0 °C, 3.0 kg per hour, and 50.0 W/cm², respectively. When the pressure of the evaporation chamber increases from 300 kPa to 1050 kPa, the ST-HS

Analysis of factors influencing the heat transfer performance of spray cooling system by lubricating oil

To analyze the impact of lubricating oil on the HTP of SCS, it is necessary to maintain other conditions unchanged. The undercooling, working fluid MFr , and HFd have been controlled at 15 °C, 3.0 kg per hour, and 30.0 W/cm², only changing the LOC.

Figures 11(a) and 11(b) show the changes in surface temperature and HTC-HS as a function of LOC. When the LOC is 1%, the ST-HS and HTC-HS are 34.23 °C and 15.12 × 10³ W/m²°C, respectively. When the LOC is 6%, the ST-HS is 60.02 °C, and the HTC is 7.48 × 10³ W/m²°C. When the LOC is 3.5%, the ST-HS is 50.01 °C, and the HTC is 10.05 × 10³ W/m²°C. When the LOC is 5%, the ST-HS is 58.22 °C, and the HTC is 7.63 × 10³ W/m²°C. Figure 11 indicates that as LOC rises, ST-HS increases while HTC decreases, resulting in a decline in SCS HTP. To examine the impact of working fluid-flow rate and lubricating oil on SCS HTP, HFd and under-cooling were set at 50.0 W/cm² and 15 °C, respectively.

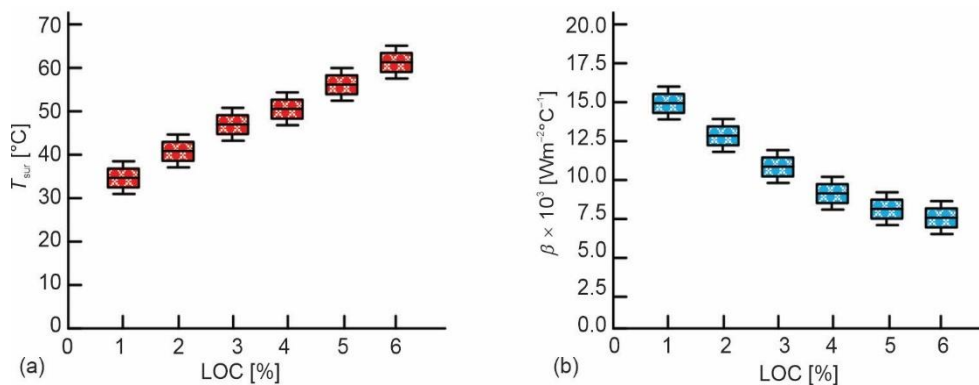


Figure 11. Effect of LOC on HTP; (a) effect of LOC on surface temperature of heat source and (b) effect of LOC on heat transfer

Figures 12(a) and 12(b) show the variation curves of the influence of five LOC on the ST-HS and HTC-HS under different MFr . When the LOC is 0.00% and the MFr increases from 1.0 kg per hour to 5.0 kg per hour, the ST-HS decreases from 69.02 °C to 36.89 °C, and the HTC increases from 8.45 × 10³ W/m²°C to 19.21 × 10³ W/m²°C. When the LOC is 0.74%, during the process of increasing the MFr from 1.0 kg per hour to 5.0 kg per hour, the ST-HS decreases from 74.23 °C to 40.05 °C, and the HTC increases from 7.02 × 10³ W/m²°C to 14.12 × 10³ W/m²°C. The HTC at a mass concentration of 1.0 kg per hour are 7.01 × 10³ W/m²°C, 7.08 × 10³ W/m²°C, and 7.10 × 10³ W/m²°C, respectively. The HTC at a mass concentration of 5.0 kg per hour are 9.02 × 10³ W/m²°C, 8.03 × 10³ W/m²°C, and 7.21 × 10³ W/m²°C, respectively. At low LOC, increasing MFr decreases ST-HS and increases HTC. At high LOC, raising MFr enhances OFT, improving HTP until a critical thickness. Beyond that, more MFr increases OFT, reducing SCS HTP. The final OFT reaches a limit, minimizing HTP. Further MFr increase then enhances overall HTE.

Figure 13 shows the effect of lubricating oil on HTP under different heat flux densities at a constant MFr of 5.0 kg per hour. Figures 13(a) and 13(b) show the results of the ST-HS and HTC-HS as the concentration of five lubricating oils changes with HFd . When the LOC is fixed at 1.47%, during the process of increasing the HFd from 10 W/cm² to 50 W/cm², the ST-HS increases from 32.33 °C to 55.28 °C, and the HTC increases from 7.54 × 10³ W/m²°C to

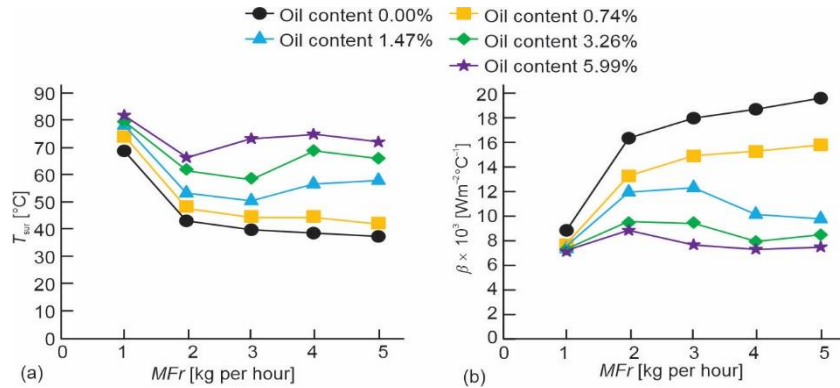


Figure 12. Effect of LOC on HTP under different MFRs;
(a) effect of oil content on surface temperature of heat source under different MFR
and (b) effect of oil content on HTC under different MFR

$9.46 \times 10^3 \text{ W/m}^2\text{°C}$. When the LOC was 0.00%, 0.74%, 3.26%, and 5.99%, the changes of ST-HS and HTC-HS maintained an upward trend in general, although the increase amplitude was different, and the change rule was consistent with that of LOC 1.47%. In summary, under the same LOC conditions, the ST-HS and HTC-HS will increase with the increase of Hfd , further improving the HTP of SCS.

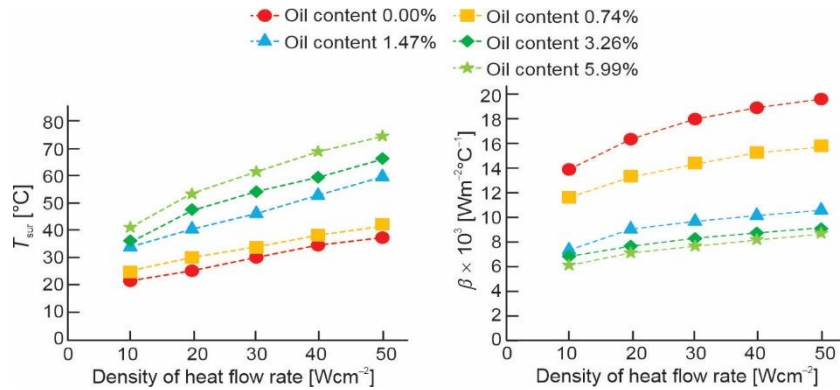


Figure 13. Effect of LOC on HTP under different HFD;
(a) effect of oil content on surface temperature of heat source under different
heat flux density and (b) effect of oil content on HTC under different HFD

Conclusion

Ships house powerful equipment generating significant heat during operation, leading to potential equipment failures and shortened service life. Addressing the crucial heat dissipation issue, traditional working fluids have limitations in flow rate and HTP. This study focuses on using SCT to tackle ship heat dissipation challenges and explores the factors influencing HTP in SCS. Research had shown that in R134a SCS, during the process of increasing MFR from 1 kg per hour to 4 kg per hour, the ST-HS decreased from 48.70 °C to 29.80 °C, and during the process of increasing flow rate from 4 kg per hour to 6 kg per hour, the temperature of the heat source increased by 3.70 °C. When the LOC was fixed at 0.74% and the MFR was 1 kg per

hour, the ST-HS and HTC-HS were $74.23\text{ }^{\circ}\text{C}$ and $7.02 \times 10^3\text{ W/m}^2\text{ }^{\circ}\text{C}$, respectively. When the MFr was 5 kg per hour, the ST-HS decreased by $34.18\text{ }^{\circ}\text{C}$ and the HTC was $14.12 \times 10^3\text{ W/m}^2\text{ }^{\circ}\text{C}$. In conclusion, factors like mass-flow, HFd , spray chamber ECp , and under-cooling affect SCS HTP to varying degrees. Under-cooling has a less noticeable impact. The presence of lubricating oil forms an oil film on the SoHS, increasing heat transfer resistance and reducing capacity. Research gaps exist, especially in understanding how MFr and HFd influence the surface liquid film in the presence of an oil film, requiring further investigation for oil content variations.

Fundings

The research is supported by: General Project of Basic Science (Natural Science) Research in Jiangsu Universities Project No.: 22KJD580001 Project Name: Experimental and Simulation Research on SCS of High-Power Warship Cooling Elements.

Reference

- [1] Chen, Z., Research on Internet Security Situation Awareness Prediction Technology Based on Improved RBF Neural Network Algorithm, *JCCE.*, 1 (2022), 3, pp. 103-108
- [2] Zhang, Y., et al., Numerical Study on the Heat Dissipation Effect of the Water-Cooled Structure of the Lateral Flange on the Pulsed Strong Magnetic Coil, *IEEE Transactions on Plasma Science*, 51, (2023), 6, pp. 1560-1567
- [3] Zhang, Z., et al., Adaptive Privacy-Preserving Federated Learning for Fault Diagnosis in Internet of Ships, *IEEE Internet of Things Journal*, 9 (2022), 9, pp. 6844-6854
- [4] Zhong, K., et al., Data-Driven Based Fault Prognosis for Industrial Systems: A Concise Overview, *IEEE/CAA Journal of Automatica Sinica*, 7 (2020), 2, pp. 330-345
- [5] Cornils, E., et al., Experimental Approach of Photovoltaic System in Operation for Performance Prediction of Natural Convection, *IEEE Latin America Transactions*, 18 (2020), 04, pp. 652-658
- [6] Garelli, N., et al., A Transient 3-D CFD Model for the Simulation of Forced or Natural Convection of the EU DEMO In-Vessel Components, *IEEE Transactions on Plasma Science*, 50 (2022), 11, pp. 4472-4480
- [7] Shams Ghahfarokhi, P., et al., The Oil Spray Cooling System of Automotive Traction Motors: The State of the Art, *IEEE Transactions on Transportation Electrification*, 9 (2023), 1, pp. 428-451
- [8] Wang, R., et al., Comparison of Heat Transfer Characteristics of the Hollow-Shaft Oil Cooling System for High-Speed Permanent Magnet Synchronous Machines, *IEEE Transactions on Industry Applications.*, 58 (2022), 5, pp. 6081-6092
- [9] Liu, C., et al., Numerical Investigation of Heat Transfer in Open Micro-channel Heat Sinks with Transverse Ribs for High Heat Flux Dissipation, *IEEE Transactions on Plasma Science.*, 50 (2022), 11, pp. 4220-4225
- [10] Clark, M. D., et al., Impact of Pressure Drop Oscillations on Surface Temperature and Critical Heat Flux During Flow Boiling in a Micro-channel, *IEEE Transactions on Components, Packaging and Manufacturing Technology*, 11 (2021), 10, pp. 1634-1644
- [11] Klinkhamer, C., et al., Jet Impingement Heat Sinks with Application Toward Power Electronics Cooling: A Review, *IEEE Transactions on Components, Packaging and Manufacturing Technology*, 13 (2023), 6, pp. 765-787
- [12] Wu, T. T., et al., Research on Spray Cooling Performance Based on Battery Thermal Management, *Int. J. Energ. Res.*, 46 (2022), 7, pp. 8977-8988
- [13] Chang, T. B., et al., Experimental Investigation into Spray Cooling Heat Transfer Performance of Al_2O_3 -Water Nanofluid with Different Subcooling Degrees, *P. I. Mech. Eng. J.-J. Eng. Part E: Journal of Process Mechanical Engineering*, 236 (2022), 2, pp. 245-253
- [14] Huang, J. L., et al., Experimental Investigation of Spray Cooling Performance in Non-Boiling Zone on Rough Super Hydrophilic/Hydrophobic Surfaces, *Int. J. Energ. Res.*, 46 (2022), 14, pp. 19566-19573
- [15] Dreo, R., et al., Detection and Localization of Multiple Ships Using Acoustic Vector Sensors on Buoyancy Gliders: Practical Design Considerations and Experimental Verifications, *IEEE Journal of Oceanic Engineering*, 48 (2023), 2, pp. 577-591
- [16] Wu, S., et al., Cooling System Design and Thermal Analysis of Modular Stator Hybrid Excitation Synchronous Motor, *CES Transactions on Electrical Machines and Systems*, 6 (2022), 3, pp. 241-251

- [17] Zhao, B., *et al.*, Model Predictive Control of Solar PV-Powered Ice-Storage Air-Conditioning System Considering Forecast Uncertainties, *IEEE Transactions on Sustainable Energy*, 12 (2021), 3, pp. 1672-1683
- [18] Wei, Q., *et al.*, Learning Control for Air Conditioning Systems via Human Expressions, *IEEE Transactions on Industrial Electronics*, 68 (2021), 8, pp. 7662-7671
- [19] Lim, J. H., Park, M., Studies on Heat Transfer Coefficient of a Circular Tube with Twisted Tape Insert for High Heat Flux Cooling Applications, *IEEE Transactions on Plasma Science*, 50 (2022), 2, pp. 459-469
- [20] van Erp, R., *et al.*, Efficient Micro-channel Cooling of Multiple Power Devices with Compact Flow Distribution for High Power-Density Converters, *IEEE Transactions on Power Electronics*, 35 (2020), 7, pp. 7235-7245